Carbohydrate Polymers 85 (2011) 726–732

Contents lists available at ScienceDirect

Carbohydrate Polymers

journal homepage: www.elsevier.com/locate/carbpol

An electrode of quartz crystal microbalance decorated with CNT/chitosan/fibronectin for investigating early adhesion and deforming morphology of rat mesenchymal stem cells

Tze-Wen Chung[a,*], Thitima Limpanichpakdee[a], Ming-Hui Yang[a], Yu-Chang Tyan[b]

[a] Department of Chemical and Material Engineering, National Yunlin University of Science and Technology, 123 University Road, Section 3, Douliou, Yunlin 640, Taiwan, ROC
[b] National Sun Yat-Sen University – Kaohsiung Medical University Joint Research Center and Department of Medical Imaging and Radiological Sciences, Kaohsiung Medical University, Kaohsiung, Taiwan, ROC

ARTICLE INFO

Article history:
Received 2 December 2010
Received in revised form 7 March 2011
Accepted 12 March 2011
Available online 2 April 2011

Keywords:
Chitosan
Hyaluronic acid
Fibronectin
Rat mesenchymal stem cells
Quartz crystal microbalance

ABSTRACT

The early responses of mesenchymal stem cells (MSCs) to various biopolymers are important to their proliferation and differentiation. Here, the adhesions of rat MSCs on the electrode of quartz crystal microbalance (QCM) decorated with multi-walled carbon nanotubes (CNT)/chitosan (CS), CNT/CS/hyaluronic acid (HA) and CNT/CS/fibronectin (FN) layers were investigated and compared with other techniques at a serum-free condition for 12-h incubation. The numbers of adhered rMSCs on CNT/CS/FN and CNT electrodes were 76 and 26% of the initial values, respectively, determined by cell-count technique while MTS assay could not detect the differences. The weights of adhered rMSCs on CNT/CS/FN electrodes of QCM were 50% higher than those on other surfaces that were consistent with cell-count technique. The morphology of adhered rMSCs on the CNT/CS/FN surfaces markedly differed from those on other surfaces. In conclusion, the electrodes of QCM decorated with CNT/CS/FN or CNT/CS/carbohydrate polymers could be quantified the early adhesion of rMSCs on their surfaces.

1. Introduction

Chitosan (CS) is a bioactive carbohydrate polymer and promising biomaterial in applications of wound healing and tissue engineering (Chung, Wang, Wang, Hsieh, & Fu, 2008; Muzzarelli, 2009, 2011). For instance, chitosan has a chemo-attraction property to initiate wound healing process or a high capacity to form complexes with both inorganic and biochemical substances for tissue engineering in bone regeneration (Muzzarelli, 2009, 2011). Chitosan grafting onto polycaprolactone (PCL) as a scaffold can enhance growth rates of fibroblasts or PC12 cells in a biomaterials of nerve conduit (Chung et al., 2008, 2011). Moreover, incorporating other molecules or polymers into chitosan to fabricate multifunctional biomaterials has been widely studied (Chung, Lu, Wang, Lin, & Chu, 2002; Muzzarelli, 2011; Yang et al., 2009). For example, the arginine-glycine-aspartic acid (RGD) peptide has been grafted onto CS films to enhance endothelial cell proliferation (Chung et al., 2002). Silk fibroin blended with chitosan as a cardiomyogenic patch significantly enhanced on proliferation of rat mesenchymal stem cells (rMSCs) (Yang et al., 2009). Recently, a cardiomyogenic patch fabricated by blending silk, chitosan and hyaluronic acid (HA) highly promoted the differentiation of rMSCs to cardiomyocytes after they were induced by 5-azacytidine (Yang et al., 2010). The favorable properties of hyaluronic acid as a biopolymer for applying in regenerative medicine have also been stated (Muzzarelli, 2011). Therefore, it is of interesting to investigate the early adhesion and the morphology of stem cells responses to the surfaces of CS or CS/HA polymers.

Fibronectin (FN), a large (450 kDa) and an abundant glycoprotein of ECM and plasma, is a multifunctional protein that supports cell attachment and adhesion (Gerecht et al., 2007) mediated by Arg-Gly-Asp-Ser peptides in an FN structure. Moreover, FN molecules were largely expressed to inter-connect rMSCs when they were differentiated to cardiomyocytes on cardiac patches (Dolatshahi-Pirouz, Jensen, Foss, Chevallier, & Besenbacher, 2009; Yang et al., 2010). Therefore, it is interesting to investigate the early responses of rMSCs to FN proteins such as cell adhesion.

QCM is an instrument that determines the adhesion of mass on a quartz sensing electrodes via measuring the responses of the frequency shifts of the electrodes due to mass changes (Kanazawa & Gordon, 1985). QCM has been widely studied to monitor immunological reactions (Cooper & Singleton, 2007) and to investigate cell-substrate interactions (Fujisaki & Hattori, 2002; Li, Thielemann, Reuning, & Johannsmann, 2005). For instance, the adhesion of human ovarian cancer cells to various extra-cellular matrix proteins has been reported (Li et al., 2005). QCM technique was

* Corresponding author. Tel.: +886 5 534 2601x4610; fax: +886 5 531 2071.
E-mail address: twchung@yuntech.edu.tw (T.-W. Chung).

0144-8617/$ – see front matter © 2011 Elsevier Ltd. All rights reserved.
doi:10.1016/j.carbpol.2011.03.025

adopted herein by modifying the sensing electrodes with chitosan and other biopolymers to quantify the amounts of cell adhesion on their surfaces.

CNT has a large surface area which has been widely studied for various purposes (Wang, 2009; Zhang, Su, & Mao, 2006). In this study, to increase the surface areas of the electrode of QCM and the amount of biopolymers such as CS to be absorbed onto the electrode of QCM, acid-treated CNT, which contain carboxylic molecules, were first dispersed onto the electrode using a surfactant (Wang, 2009). Then, the CNT/CS, CNT/CS/HA and CNT/CS/FN electrode surfaces were fabricated via the layer-by- layer technique for this study.

Mesenchymal stem cells (MSCs) are a promising cell for tissue engineering as they are a potential source of cells for therapeutic strategies. Notably, MSCs have an intrinsic ability to re-generate and differentiate into several functional cells, including muscle and adipose cells (Baksh, Song, & Tuan, 2004; Chen, Rousche, & Tuan, 2006). Therefore, applications of MSCs in regenerative medicine using an animal model have been demonstrated for regeneration of bone, cardiomyocytes, and neurons (Chamberlain et al., 2004; Grinnemo et al., 2004; Muzzarelli, 2011; Sugaya, 2003). However, the investigation of early responses of rMSCs to various biopolymers such as CNT/CS/FN surfaces under serum-free conditions is lacking. To study the issue, the surfaces of electrodes of a QCM decorated with CNT/CS, CNT/CS/HA and CNT/CS/FN layers were first fabricated via a layer-by-layer technique. The QCM with the decorating electrodes was utilized to quantify the mass of rMSCs adhered on the electrodes after they were incubated with the cells for 12 h in a serum-free medium. The frequency shifts or mass of adhered rMSCs on the aforementioned surfaces were measured, calculated, and the results were compared with those determined by cell counting technique and cell viability assay (MTS). Moreover, the morphology of rMSCs responses to those decorating surfaces was observed by a confocal microscopy at the same conditions as those in QCM measurements. Interestingly, the adhesions and morphology changes of rMSCs to biopolymer surfaces are fast, and can be determined via QCM technique and observed via confocal microscopy, respectively.

2. Materials and methods

2.1. Reagents and solutions

Multi-walled carbon nanotubes (MWCNT, 6–13 nM outer diameter, 2.5–20 μm long) with a purity of 99%, rat fibronectin, 4′-6-diamidino-2-phenylindole (DAPI), and Quinacrin dihydrochoride were provided by Sigma, St Louis, MO, USA. Pluronic F-68, Minimum Essential Medium (MEM) Alpha Medium (1X), and Fetal Bovine Serum (FBS) were all purchased from Invitrogen, USA. Chitosan (low molecular weight with viscosity of 20,000 cps and 75–85% deacetylated) was purchased from Aldrich, Milwaukee, WI, USA. Hyaluronic acid (M.W. 15 kDa) was purchased from Lifecore Biomedical, Inc., MN, USA. All chemicals were analytical grade. Moreover, 1% CS was prepared in acetic acid solution; 0.5% HA and 50 mg/ml FN was prepared in phosphate-buffered saline (PBS) solution.

2.2. Fabricating CNT and dispersing CNT on the electrode of a QCM

The CNT were treated by refluxing in concentrated nitric acid at 85 °C for 3 h. When the CNT precipitated from the solution, the nitric acid was carefully removed. The mixture was then filtered through a 0.22-μm filter under a vacuum condition. The CNT were washed with D.I. water, collected and dried in an oven at 50 °C.

The surface of a 9-MHz QCM gold electrode (ANT Tech, Taiwan) was washed with 1 M HCl, rinsed with water, followed by drying at room temperature. The frequency of the electrode measured by the QCM (ADS, ANT Tech, Taiwan) was assigned as F_0 at the flow rate was 60 μL/min of PBS. For preparing an electrode with CNT decoration, a solution of pluronic F68 was applied to disperse CNT on the electrode surface (Wang, 2009). Briefly, 1% F68 solution was dropped onto the gold electrode of a QCM and then dried with slowly shaking. CNT in solution was then deposited on the surface of the electrode and dried for further applications.

2.3. Adsorption of chitosan, chitosan/hyaluronic acid, chitosan/fibronectin onto CNT surfaces determined by QCM measurements and characterized FT-IR

For fabricating a CNT/CS electrode, 0.5% of CS solution was injected into the flow loop with a CNT dispersing electrode at the flow rate was 60 μL/min and the frequency shifts of the QCM were measured. Moreover, two times injections of CS solution were performed to assure that the adsorption of CS on the electrode was in a saturation condition. The frequency shifts (ΔF) determined by the QCM were recorded and the mass of CS adsorption were calculated. To test CNT/CS layer stably coated onto the electrode, the frequency of the electrode was measured by flow of PBS for several minutes.

To fabricate CNT/CS/HA coating electrode, 0.5% HA solution was injected into the flow loop of the QCM equipped with CNT/CS electrode. HA polymers were adsorbed onto the CS layer by ionic interactions which would result in frequency shifts of the QCM. The same steps as those for preparing CNT/CS electrodes were performed for fabricating CNT/CS/HA electrode. For preparing an electrode decorated by CNT/CS/FN, the same steps as those for preparing CNT/CS/HA electrodes were performed by injecting 50 mg/mL FN solution into flow loop. Two more injections of FN might be performed to assure the saturation status of CNT/CS/FN on the electrode. All frequency changes of decorated layers on the electrodes of QCM were calculated to determine the adsorbed mass of biopolymers using the Kanazawa model (Kanazawa & Gordon, 1985).

The surface morphology of the electrode decorated with CNT was observed using a scanning electron microscope (JEOL JSM-6700F, Tokyo, Japan). Moreover, Fourier transform infrared spectra (FT-IR) of CNT, CNT/CS, CNT/CS/HA, and CNT/CS/FN layers were determined using a FT-IR spectrometer (PerkinElmer, Spectrum One system, USA).

2.4. Culturing rMSCs on the electrodes decorated by CNT, CNT/chitosan, CNT/chitosan/hyaluronic acid, and CNT/chitosan/fibronectin surfaces

For seeding rMSCs, the CNT electrodes decorated by various biopolymer layers except for CNT/CS/FN were sterilized with 70% (v/v) ethanol and then exposed at ultraviolet light. 4×10^4 rMSCs in serum-free medium was added to each well in presence of the aforementioned electrodes and incubated at 37 °C in 5% CO_2 for 12 h (Chung et al., 2011; Yang et al., 2009) for investigating the adhesion of the cells on those electrodes. After the incubations, the electrodes were washed with PBS, and then frequency shifts were measured by the QCM at a flow rate of 60 μL/min of PBS to quantify the adhesions of rMSCs on electrodes.

2.5. Counting the numbers and MTS assay of the adhered rMSCs on the electrodes decorated by CNT/chitosan and other biopolymers

For counting the numbers of adhered rMSCs on the aforementioned electrodes after incubation, the electrodes were washed and

fixed with 4% formaldehyde. The nuclei of the cells were stained with 4′-6-diamidino-2-phenylindole (DAPI), and observed by a microscope equipped with fluorescence light source (Nikon TE-100, Japan), and the micrographs were taken with a CCD camera (Chung et al., 2011; Yang et al., 2009). The nucleuses of cells were counted by Image pro plus 6. In addition, the viability of the adhered cells was determined by MTS assay (CellTiter 96® Aqueous One Solution Proliferation Assay). The detailed procedures were followed to our earlier reports (Chung et al., 2011; Yang et al., 2009). In brief, the samples were incubated with 200 μL medium/MTS solutions for 4 h at 37 °C. The absorbance of formazan solutions of each sample was measured by an ELISA micro-plate reader at 570 nm (ELx800, Bio-Tek Instruments, Inc., Winooski, VT, USA).

2.6. Cell morphology of rMSCs on various surfaces observed by immuno-chemical straining

For immunochemical staining of the morphology of adhered rMSCs via a confocal microscope (Yang et al., 2009), the same components as the electrodes were prepared on cover slips and were incubated for 12 h at the same conditions as those on the aforementioned electrodes. For studying the possibly deforming the morphology of adhered rMSCs on surfaces of the cover slips (e.g. CNT/CS/FN surfaces), the cover slips were rinsed by PBS and fixed in 10% formaldehyde (Sigma–Aldrich, USA) at 4 °C (Chung et al., 2011; Yang et al., 2009). The samples were also blocked with 2% bovine serum albumin (BSA) (Sigma–Aldrich, USA). The cells were incubated with anti-vimentin (mouse IgG, anti-rat 1:200) (Chemicon. CA, USA) and subsequently incubated with appropriate secondary antibody (Alexa Fluor 488) (Molecular Probes, Invitrogen, USA). The samples were then incubated with DAPI to stain nuclei of the cells. Cells were visualized and their images were taken using a laser confocal microscopy (LCSM, Zeiss Inverted LSM-410, Zeiss optical company, Germany) (Chung et al., 2011; Yang et al., 2009). Cells were performed without adding the primary antibodies assigned as a control group.

All calculations used the SigmaStat statistical software (Jandel Science Corp., San Rafael, CA). Statistical significance was evaluated at 95% of confidence level or better. Data are presented as mean ± S.D.

3. Results and discussion

3.1. Characterizations of electrodes of QCM decorated with CNT, CNT/chitosan, CNT/chitosan/hyaluronic acid, and CNT/chitosan/fibronectin

In this study, acidic CNT with COOH groups were dispersed on the surface of the gold electrode of the QCM to increase the surface areas of the electrode, and the amounts of biopolymers (e.g. CS and CS/FN) adsorption onto the electrode for subsequent applications. To achieve a homogeneous dispersion of CNT on a QCM electrode, 1% w/w F68 was coated onto the surface of an electrode (Wang, 2009) that could well disperse acidic CNT on it (Fig. 1). Conversely, CNT were highly aggregated on the electrode surface without F68 treatment (data not shown).

To investigate frequency shifts for deposition of various biopolymers, such as CS, HA, and FN, on QCM electrode surfaces, the absorption of a specific biopolymer (e.g., HA and FN) onto a CNT decorating electrode surface was attained using a layer-by-layer technique. The frequencies dropped sharply for all tested biopolymers, indicating that they were absorbed onto the electrode surfaces (Fig. 2a), as has been reported by other studies (Marx, 2003). Table 1 shows frequency responses for the biopolymers (e.g., CNT/CS and CNT/CS/HA). The mass of those biopolymers was cal-

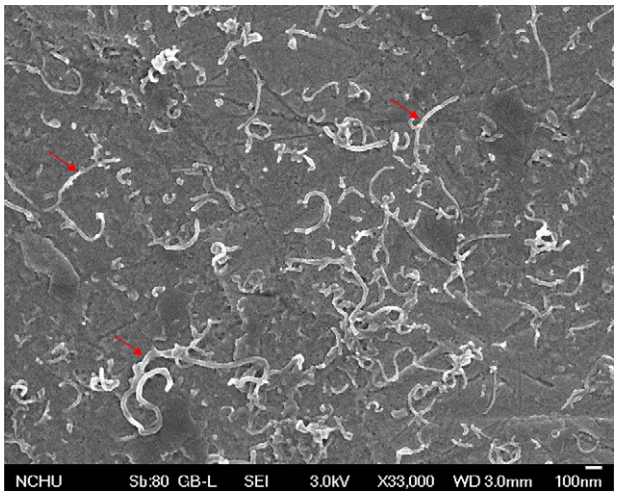

Fig. 1. SEM images of a QCM electrode coated with CNT at a magnification of 30,000× (red arrows point to CNT tubes). (For interpretation of the references to color in this figure legend, the reader is referred to the web version of the article.)

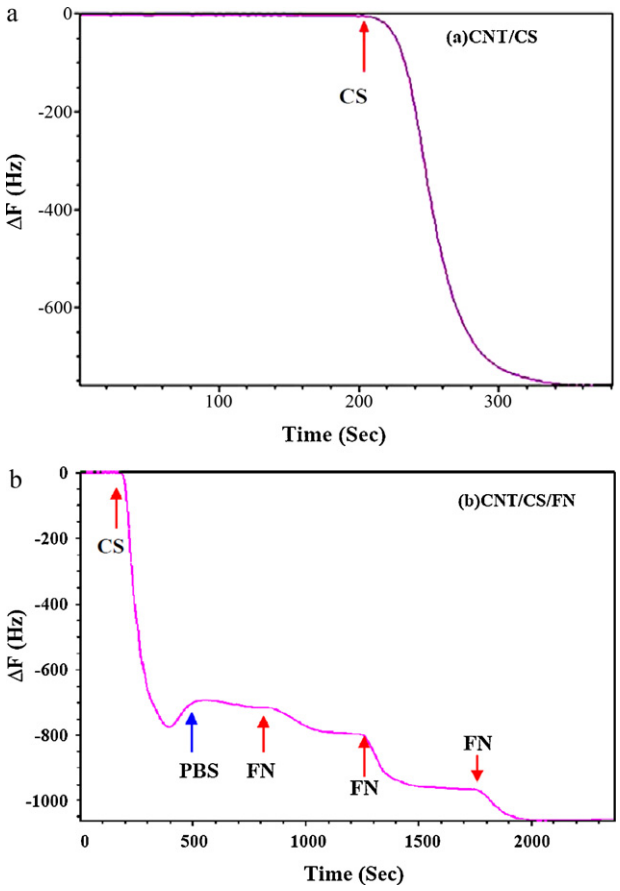

Fig. 2. Frequency shifts for preparing the electrodes decorated with (a) CNT/CS and (b) CNT/CS/FN layers.

Table 1
Frequency shifts and mass for the adsorption of CNT, CNT/CS, CNT/CS/HA, and CNT/CS/FN layers measured by the QCM and calculated by the Sauerbrey equation.

Absorption polymer	ΔF (Hz)	Δm (ng)
CNT	−2004 ± 33	−1393 ± 100
CS	−732 ± 24	503 ± 16
HA	−1276 ± 70	873 ± 45
FN	−1040 ± 20	714 ± 14

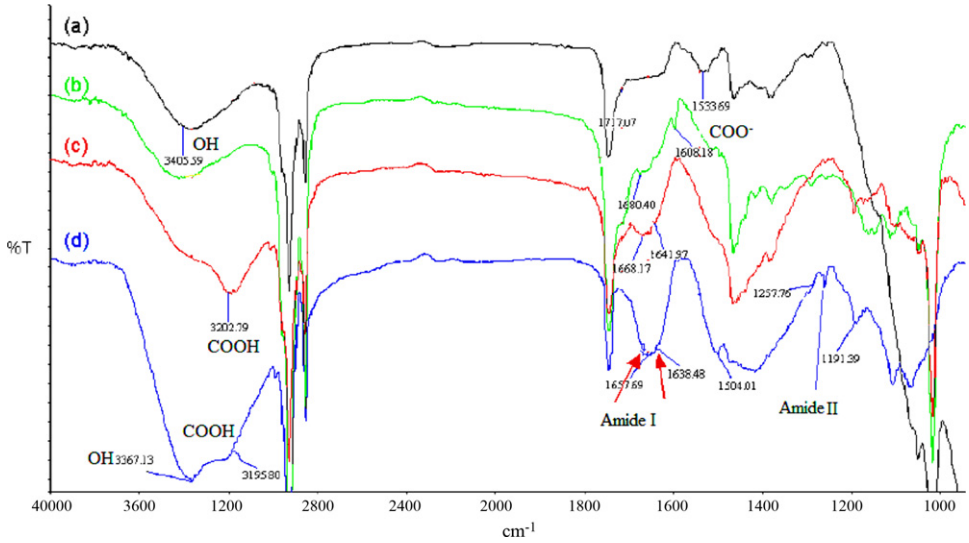

Fig. 3. The ATR-FTIR transmission spectra of (a) CNT, (b) CNT/CS, (c) CNT/CS/HA, and (d) CNT/CS/FN layers decorated on electrodes of QCM.

culated using the Sauerbrey equation (Kanazawa & Gordon, 1985). These results demonstrate that various biopolymers were successfully coated onto CNT layers via the layer-by-layer technique. Among those depositions, CNT has the highest frequency responses and mass depositions on the electrode (e.g., 1393 ± 100 ng, $n = 5$) (Table 1) while CS has the lowest frequency responses (e.g., 732 ± 24 ng, $n = 5$). The absorption of CNT on the electrode could increase its surface area to enhance absorption of CS onto the electrode and, consequently, increase the sensitivity of QCM. Moreover, the amount of the adsorption of CS without CNT deposition was much less than that with in presence of CNT (data not shown). Interestingly, FN needed three injections to reach the saturation state of FN on the CNT/CS surfaces (Fig. 2b). It may be due to that FN is a protein with a complex structure and relatively high molecular weight, resulting in un-stable adhesion to CS polymers and the needs for multiple FN injections.

Fig. 3 shows the characteristics of the aforementioned polymers of FT-IR spectra. For the absorption curve of the absorptions of CNT spectra (the curve A), a broad band at 3406 cm^{-1} was attributed to the OH functional group from F68, a disperse agent for CNT, due to the polyethylene oxide (PEO)–polypropylene oxide structure (Wang, 2009). Moreover, an absorption band at 1717 cm^{-1} can be attributed to stretching vibration of C=O, and the wave numbers at 1610–1530 were the adsorption band of COO^- symmetrical stretching which are attributed by acid treatment of CNT (Zhang et al., 2006). Absorption bands at 3405 and 1680 cm^{-1} for the curve B correspond to a primary OH from CS. The new absorbance at 1608 cm^{-1} indicates the presences of amide groups of CS (Bakota, Aulisa, Tsyboulski, Weisman, & Hartgerink, 2009). For the curve C, a strong band at 3202 cm^{-1} for OH from a carboxylic group is due to the addition of HA and the C=O absorption band at 1668 and 1642 cm^{-1} due to the interactions of amino and carboxyl groups (Bakota et al., 2009). The bands at 1658 and 1638 cm^{-1} show the presences of amide I of FN (Koteliansky et al., 1981; Li et al., 2008). The weak signal at 1257 cm^{-1} represents amide III of FN (Koteliansky et al., 1981) while the amide II bands (e.g., 1520 and 1550 cm^{-1}) were weak and may be hindered by signals from CS. These spectra indicated that the electrodes were successfully decorated with CNT, CNT/CS, CNT/CS/HA, and CNT/CS/FN biopolymers.

3.2. Quantitative the adhesions of rMSCs on the electrodes of QCM by counting cell and QCM techniques

To investigate the adhesion of rMSCs onto the electrodes decorated by CNT, CNT/CS, CNT/CS/HA, and CNT/CS/FN layers, rMSCs were incubated with the electrodes for 12 h. Moreover, since the adsorption of various proteins of bovine serum onto the aforementioned surfaces may influence cell adsorption behaviors, serum-free medium in cell cultural were employed herein. Additionally, 12-h cultivation of rMSCs under serum-free conditions used herein might not result in apoptosis or proliferation of cells (Pochampally, 2004). Besides QCM technique, the numbers of the adhesive rMSCs on the aforementioned surfaces was determined by counting the nucleus of the cells stained by DAPI. According to calculations of the adhered cells on the electrodes obtained in micrographs, the number of adhered rMSCs on the CNT/CS/FN coating surface was significantly higher than those for other surfaces (e.g., $76 \pm 24\%$ and 26–46% of original cell counts, Table 2, $n = 4$, respectively). Ode et al. (2010) reported that coated FN on culture plates enhances adhesion, migration, and proliferation of rMSCs under a low-serum condition. Notably, since serum-free medium was adopted in this study, interactions between rMSCs and FN may be due to interactions among glycoprotein domains on the membrane surfaces of rMSCs and RGD peptide sequences of FN (Hynes, 1992).

In addition to the cell counting method via DAPI stain for evaluating adhesions of rMSC to the surfaces of electrodes decorated by aforementioned biopolymers, the same experimental settings were also adopted for cell viability evaluated by MTS assay and fre-

Table 2
Cell numbers of adhered rMSCs on the electrodes decorated with CNT, CNT/CS, CNT/CS/HA, and CNT/CS/FN biopolymers for 12 h of cell incubation, determined by calculating the micrographs taken from a fluorescent microscopy.

Biopolymer surfaces	CNT	CNT/CS	CNT/CS/HA	CNT/CS/FN
Cell density ($1 \times 10^4/cm^2$)	$0.77 \pm 0.36^*$	1.32 ± 0.09	$1.18 \pm 0.20^\#$	$2.19 \pm 0.17^{*,\#}$

* $P < 0.001$, CNT vs. CNT/CS/FN.
$^\#$ $P < 0.05$, CNT/CS/HA vs. CNT/CS/FN, $n = 4$.

Table 3
Frequency shifts of QCM and weights of adhered rMSCs on the electrodes decorated with CNT, CNT/CS, CNT/CS/HA and CNT/CS/FN layers for 12 h of cell incubation.

Biopolymer surface	CNT	CNT/CS	CNT/CS/HA	CNT/CS/FN
ΔF (Hz)	$-6196 \pm 380^{*}$	$-7180 \pm 360^{*}$	$-6994 \pm 511^{\#}$	$-9224 \pm 494^{\#}$
Weight of adhered rMSCs (ng)	$4236 \pm 261^{*}$	$5162 \pm 456^{*}$	$4799 \pm 364^{\#}$	$6337 \pm 339^{\#}$

* $P < 0.001$, CNT vs. CNT/CS/FN.
$^{\#}$ $P < 0.001$, CNT/CS/HA vs. CNT/CS/FN, $n = 4$.

quency shifts via QCM measurements. The MTS assay measures the mitochondrial metabolic rate of cells that have been applied widely for biomaterial researches (Chung et al., 2008; Fujisaki & Hattori, 2002). However, no significant difference existed in the results MTS assay among the aforementioned surfaces (e.g., CNT/CS/FN layer) in this study (data not shown). No difference in results of MTS assay may be due to low cell numbers adhered to the tested surfaces, resulting in a non-sensitive assay. For instance, 4×10^4 rMSC cells were employed to evaluate the interactions between rMSCs and biopolymer surfaces of electrodes. Since the absorption percentages of cells to the surfaces were generally 26–76% (Table 2), indicating that $1.0–3.0 \times 10^4$ rMSC cells were on CNT, CNT/CS, CNT/CS/HA, and CNT/CS/FN surfaces. According to manufacturer instructions MTS assay, the assay for evaluating metabolic activity would be likely performed at 2.5×10^4 cells or more (Petty, Sutherland, Hunter, & Cree, 1995). At low cell num-

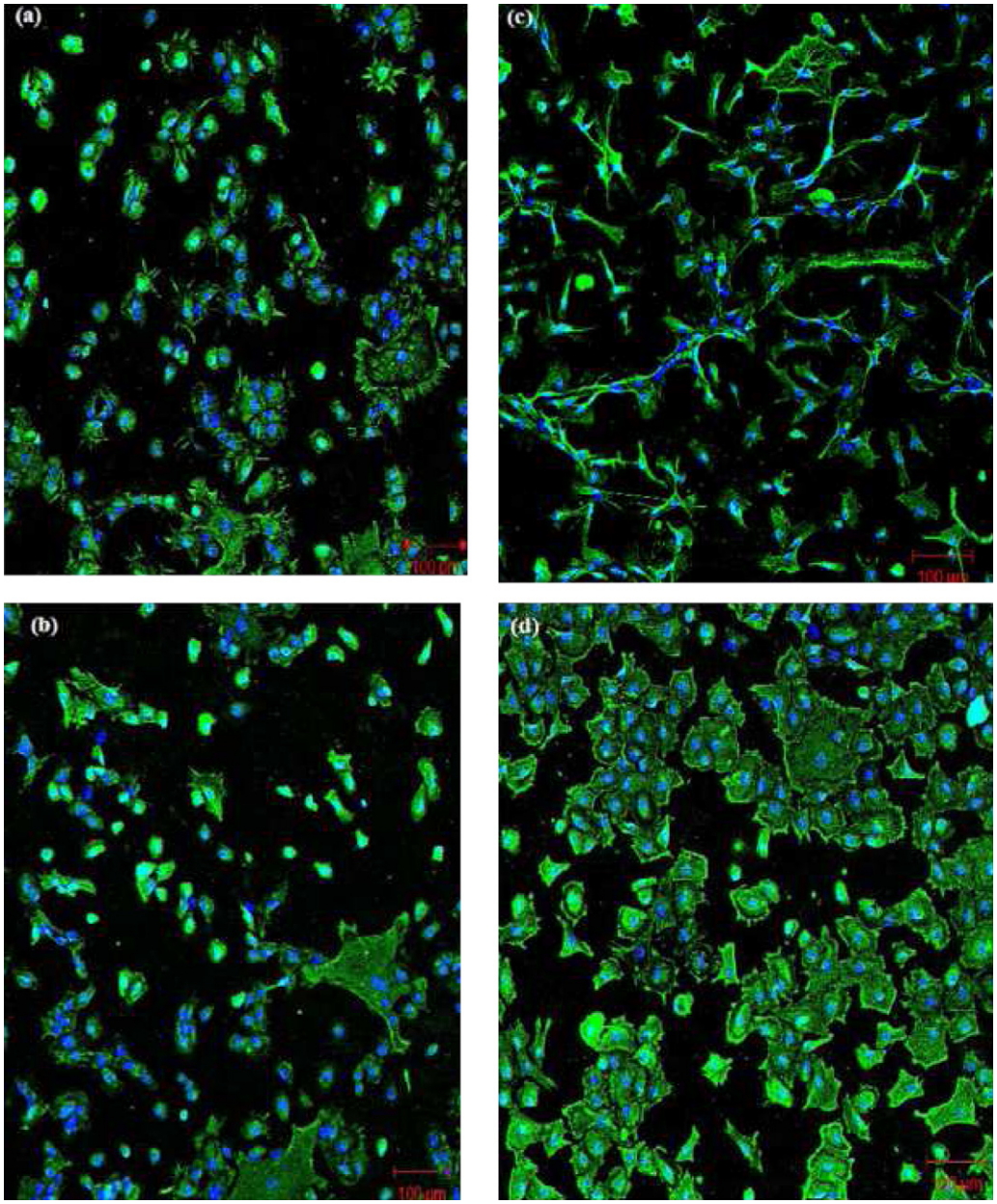

Fig. 4. Immunochemical stains for DAPI (blue) and vimentin (green) for adhered rMSCs on the electrodes decorated with (a) CNT, (b) CNT/CS, (c) CNT/CS/HA, and (d) CNT/CS/FN layers for 12 h of incubation to observe the deforming morphology of the cells. (For interpretation of the references to color in this figure legend, the reader is referred to the web version of the article.)

bers (e.g., 1.0×10^4 cells) as employed in this study, the MTS assay may be not accuracy enough to assess cell viability, consequently, no difference in determining the numbers of the adhesion of rMSCs on the electrodes.

The results of adhesion of rMSC onto the electrode of QCM decorated by CNT/CS, CNT/CS/HA and CNT/CS/FN layers were also determined by the frequency shifts as reports by other investigators in various applications (Cooper & Singleton, 2007; Li et al., 2005). The values of frequency shifts for CNT, CNT/CS, CNT/CS/HA and CNT/CS/FN coating electrodes were -6196 ± 380, -7180 ± 360, -6994 ± 511 and -9224 ± 494 Hz ($n = 4$), respectively. Moreover, the amount of rMSCs adhered onto the CNT/CS/FN coating electrode was significantly higher than others (Table 3, $P < 0.001$, $n = 4$). The mass of adhesion of rMSCs onto the CNT/CS/FN coating electrode was calculated and significantly higher than those adhered onto other surfaces such as CNT/CS surfaces (Table 3). The interactions of RGD integrin domain of FN and the receptors on the membrane receptors of rMSCs would play an important role on the adhesion study of CNT/CS/FN layers decorating electrodes as reported by others (Li et al., 2005) although these two studies employed different conditions for cell cultivation. In this study, the results of cell count and QCM techniques employed to investigate adhesions of rMSCs to various polymer surfaces coating the electrodes were consistent. Notably, employing QCM technique in this study has several advantages over the cell counting technique and MTS assay; such no need for tedious labor for counting, reducing counting errors by using images of DAPI-stained cells, and avoiding using non-sensitive of MTS technique at low cell number cases, respectively.

3.3. Morphology of adhered rMSCs on CNT/chitosan/hyaluronic acid and CNT/chitosan/fibronectin layers observed by immunochemical staining

Since various percentages of adhered rMSCs on various surfaces coating electrodes within the 12 h cultivation period (e.g., 76% of initial rMSCs adhesion on the electrodes decorated by CNT/CS/FN layers), monitoring cell morphology on those surfaces using a confocal microscopy is of interest. For these observations, CNT, CNT/CS, CNT/CS/HA and CNT/CS/FN layers were first fabricated on glass slips and rMSCs were seeded on those surfaces. Fig. 4 shows the morphology of rMSCs adhered onto those polymer surfaces with DAPI and vimentin staining (Cooper & Singleton, 2007; Yang et al., 2010). The rMSCs adhered to CNT surfaces that formed varying cell morphology (Fig. 4a). For example, parts of adhered cells were spread out on the surface while many of them were not. This is possibly due to the heterogeneous dispersion of CNT on the coating surface for cell adhesions (Fig. 1). However, the detailed mechanisms warrant further investigation. Similar morphological results of rMSCs as those for the CNT surfaces were observed in the CNT/CS case (Fig. 4b). Interestingly, the morphology of rMSCs adhered onto HA and FN surfaces differed markedly from CNT and CNT/CS surfaces (Fig. 4c and d). For instance, most adhered rMSCs on HA surfaces spread widely with a long splender projection. It has been reported that HA may help in cell growth, adhesion, migration, and proliferation (Miyazaki, Miyauchi, Nakamura, Takeshita, & Horie, 1996; Yang et al., 2010). Moreover, HA polymers enhance rMSCs to differentiate into cardiomyocytes after they were induced by 5-azacytidine which was mainly mediated by the CD44 receptors on the membrane surfaces of rMSCs (Yang et al., 2010). Of interesting, the possible interactions between HA polymers and CD44 receptors of rMSCs might happen within 12 h incubation and resulted in deforming morphological of rMSCs (Fig. 4c) since this investigation was performed under serum-free conditions.

It was reported that the fibronectin-coated substrates might modulate the MSC phenotype (Huang, Chu, Lee, & Li, 2010), which may result in deforming cell morphology of many adhered rMSCs on CNT/CS/FN surfaces (Fig. 4d) than those of CNT and CNT/CS surfaces (Fig. 4a and 4b). For example, vimentin stains of the rMSCs on CNT/CS/FN surfaces homogenously distributed and spread in cytoplasm of the cells. It is postulated that the interactions of RGD peptides of FN and $\alpha_3\beta_5$ integrin proteins of MSCs, an RGD receptor (Semon et al., 2010) play an important role on morphological deformations (Fig. 4d).

4. Conclusions

According to results of cell counting rMSCs stained with DAPI and frequency shifts determined by QCM, the numbers or mass of adhered rMSCs on the CNT/CS/FN surface of the electrodes were significantly higher than those on other surfaces. Employing CS, HA and FN decorating electrodes for investigating mass of adhered rMSCs on those surfaces could be conveniently detected by a QCM technique in a flow condition. Additionally, marked differences in deforming cell morphology for adhered rMSCs on CNT/CS/HA and CNT/CS/FN surfaces compared with those on CNT or CNT/CS surfaces were observed in 12 h cultural that might be due to interactions between the membrane receptors of rMSCs and those polymers. In conclusion, the numbers of rMSCs adhesion and deforming morphology of the cells on various biopolymer surfaces were rapid that would influence the later proliferations and differentiations of the cells to specific cell types.

Acknowledgment

The authors would like to thank the National Science Council of the Republic of China, Taiwan, for financially supporting this research.

References

Bakota, E. L., Aulisa, L., Tsyboulski, D. A., Weisman, R. B., & Hartgerink, J. D. (2009). Multidomain peptides as single-walled carbon nanotube surfactants in cell culture. *Biomacromolecules*, *10*, 2201–2206.

Baksh, D., Song, L., & Tuan, S. R. (2004). Adult mesenchymal stem cells: Characterization, differentiation, and application in cell and gene therapy. *Journal of Cellular and Molecular Medicine*, *8*, 301–316.

Chamberlain, J. R., Schwarze, U., Wang, P. R., Hirata, R. K., Hankenson, K. D., Pace, J. M., et al. (2004). Gene targeting in stem cells from individuals with osteogenesis imperfecta. *Science*, *303*, 1198–1201.

Chen, F. H., Rousche, K. T., & Tuan, R. S. (2006). Technology insight: Adult stem cells in cartilage regeneration and tissue engineering. *Nature Clinical Practice: Rheumatology*, *2*, 373–382.

Chung, T.-W., Lu, Y.-F., Wang, S.-S., Lin, Y.-S., & Chu, S.-H. (2002). Growth of human endothelial cells on photochemically grafted Gly-Arg-Gly-Asp (GRGD) chitosans. *Biomaterials*, *23*(24), 4803–4809.

Chung, T.-W., Wang, S.-S., Wang, Y.-Z., Hsieh, C.-H., & Fu, E. (2008). Enhancing growth and proliferation of human gingival fibroblasts on chitosan grafted poly (ε-caprolactone) films is influenced by nano-roughness chitosan surfaces. *Journal of Materials Science: Materials in Medicine*, *20*(1), 397–404.

Chung, T. W., Yang, M. C., Tseng, C. C., Sheu, S. H., Wang, S. S., Huang, Y. Y., et al. (2011). Promoting regeneration of peripheral nerves in-vivo using new PCL-NGF/Tirofiban nerve conduits. *Biomaterials*, *32*(3), 734–743.

Cooper, M. A., & Singleton, V. T. (2007). A survey of the 2001 to 2005 quartz crystal microbalance biosensor literature: Applications of acoustic physics to the analysis of biomolecular interactions. *Journal of Molecular Recognition*, *20*(3), 154–184.

Dolatshahi-Pirouz, A. J., Jensen, T., Foss, M., Chevallier, J., & Besenbacher, F. (2009). Enhanced surface activation of fibronectin upon adsorption on hydroxyapatite. *Langmuir*, *25*, 2971–2978.

Fujisaki, H., & Hattori, S. (2002). Keratinocyte apoptosis on type I collagen gel caused by lack of laminin 5/10/11 deposition and Akt signaling. *Experimental Cell Research*, *280*(2), 255–269.

Gerecht, S., Burdick, J. A., Ferreira, L. S., Townsend, S. A., Langer, R., & Vunjak-Novakovic, G. (2007). Hyaluronic acid hydrogel for controlled self-renewal and differentiation of human embryonic stem cells. *Proceedings of the National Academy of Sciences of the United States of America*, *104*(27), 11298–11303.

Grinnemo, K. H., Mansson, A., Dellgren, G., Klingberg, D., Wardell, E., Drvota, V., et al. (2004). Xenoreactivity and engraftment of human mesenchymal stem cells transplanted into infarcted rat myocardium. *Journal of Thoracic and Cardiovascular Surgery*, *127*, 1293–1300.

Huang, N. F., Chu, J., Lee, R. J., & Li, S. (2010). Biophysical and chemical effects of fibrin on mesenchymal stromal cell gene expression. *Acta Biomaterialia*, *6*(10), 3947–3956.

Hynes, R. O. (1992). Integrins: Versatility, modulation, and signaling in cell adhesion. *Cell*, *69*, 11–25.

Kanazawa, K. K., & Gordon, J. G., II. (1985). Frequency of a quartz microbalance in contact with liquid. *Analytical Chemistry*, *57*(8), 1770–1771.

Koteliansky, V. E., Glukhova, M. A., Bejanian, M. V., Smirnov, V. N., Filimonov, V., Zalite, V. O. M., et al. (1981). A study of the structure of fibronectin. *Federation of European Biochemical Societies*, *119*, 619–624.

Li, J., Thielemann, C., Reuning, U., & Johannsmann, D. (2005). Monitoring of integrin-mediated adhesion of human ovarian cancer cells to model protein surfaces by quartz crystal resonators: Evaluation in the impedance analysis mode. *Biosensors and Bioelectronics*, *20*(7), 1333–1340.

Li, S., Wang, F., Wang, Y., Wang, J., Ma, J., & Xiao, J. (2008). Effect of acid and TETA modification on mechanical properties of MWCNTs/epoxy composites. *Journal of Materials Science*, *43*(8), 2653–2658.

Marx, K. A. (2003). Quartz crystal microbalance: A useful tool for studying thin polymer films and complex bio-molecular systems at the solution–surface interface. *Bio-macromolecules*, *4*(5), 1099–1120.

Miyazaki, T., Miyauchi, S., Nakamura, T., Takeshita, S., & Horie, K. (1996). The effect of sodium hyaiuronate on the growth of rabbit corneal epithelial cells in vitro. *Journal of Ocular Pharmacology and Therapeutics*, *12*, 409–415.

Muzzarelli, R. A. A. (2009). Chitins and chitosans for the repair of wounded skin, nerve, cartilage and bone. *Carbohydrate Polymers*, *76*, 167–182.

Muzzarelli, R. A. A. (2011). Chitosan composites with inorganics, morphogenetic proteins and stem cells, for bone regeneration. *Carbohydrate Polymers*, *83*, 1433–1445.

Ode, A., Duda, G. N., Glaeser, J. D., Matziolis, G., Frauenschuh, S., Perka, C., et al. (2010). Toward biomimetic materials in bone regeneration: Functional behavior of mesenchymal stem cells on a broad spectrum of extracellular matrix components. *Journal of Biomedical Materials Research A*, *95*(4), 1114–1124.

Petty, R. D., Sutherland, L. A., Hunter, E. M., & Cree, I. A. (1995). Comparison of MTT and ATP-based assays for the measurement of viable cell number. *Journal of Bioluminescence and Chemiluminescence*, *10*(1), 29–34.

Pochampally, R. R. (2004). Serum deprivation of human marrow stromal cells (hMSCs) selects for a subpopulation of early progenitor cells with enhanced expression of OCT-4 and other embryonic genes. *Blood*, *103*(5), 1647–1652.

Semon, J. A., Nagy, L. H., Llamas, C. B., Tucker, H. A., Lee, R. H., & Prockop, D. J. (2010). Integrin expression and integrin-mediated adhesion in vitro of human multipotent stromal cells (MSCs) to endothelial cells from various blood vessels. *Cell and Tissue Research*, *341*(1), 147–158.

Sugaya, K. (2003). Potential use of stem cells in neuroreplacement therapies for neurodegenerative diseases. *International Review of Cytology*, *228*, 1–30.

Wang, H. (2009). Dispersing carbon nanotubes using surfactants. *Current Opinion in Colloid & Interface Science*, *14*(5), 364–371.

Yang, M.-C., Chi, N.-H., Chou, N.-K., Huang, Y.-Y., Chung, T.-W., Chang, Y.-L., et al. (2010). The influence of rat mesenchymal stem cell CD44 surface markers on cell growth, fibronectin expression, and cardiomyogenic differentiation on silk fibroin–hyaluronic acid cardiac patches. *Biomaterials*, *31*(5), 854–862.

Yang, M.-C., Wang, S.-S., Chou, N.-K., Chi, N.-H., Huang, Y.-Y., Chang, Y.-L., et al. (2009). The cardiomyogenic differentiation of rat mesenchymal stem cells on silk fibroin–polysaccharide cardiac patches in vitro. *Biomaterials*, *30*(22), 3757–3765.

Zhang, M., Su, L., & Mao, L. (2006). Surfactant functionalization of carbon nanotubes (CNT) for layer-by-layer assembling of CNT multi-layer films and fabrication of gold nanoparticle/CNT nanohybrid. *Carbon*, *44*(2), 276–283.